

A NEARLY NAKED SUPERMASSIVE BLACK HOLE

J. J. CONDON

National Radio Astronomy Observatory¹, Charlottesville, VA 22903-2475, USA

JEREMY DARLING

Center for Astrophysics and Space Astronomy, Department of Astrophysical and Planetary Sciences, University of Colorado, 389 UCB, Boulder, CO 80309-0389, USA

Y. Y. KOVALEV

Astro Space Center of Lebedev Physical Institute, Profsoyuznaya 84/32, 117997 Moscow, Russia and
Max-Planck-Institute for Radio Astronomy, Auf dem Hügel 69, D-53121, Germany

AND

L. PETROV

Astrogeo Center, 7312 Sportsman Dr, Falls Church, VA 22043, USA

Draft version November 2, 2016

ABSTRACT

During a systematic search for supermassive black holes (SMBHs) not in galactic nuclei, we identified the compact symmetric radio source B3 1715+425 with an emission-line galaxy offset ≈ 8.5 kpc from the nucleus of the brightest cluster galaxy (BCG) in the redshift $z = 0.1754$ cluster ZwCl 8193. B3 1715+425 is too bright (brightness temperature $T_b \sim 3 \times 10^{10}$ K at observing frequency $\nu = 7.6$ GHz) and too luminous (1.4 GHz luminosity $L_{1.4\text{GHz}} \sim 10^{25}$ W Hz⁻¹) to be powered by anything but a SMBH, but its host galaxy is much smaller (~ 0.9 kpc \times 0.6 kpc full width between half-maximum points) and optically fainter (R-band absolute magnitude $M_r \approx -18.2$) than any other radio galaxy. Its high radial velocity $v_r \approx 1860$ km s⁻¹ relative to the BCG, continuous ionized wake extending back to the BCG nucleus, and surrounding debris indicate that the radio galaxy was tidally shredded passing through the BCG core, leaving a nearly naked supermassive black hole fleeing from the BCG with space velocity $v \gtrsim 2000$ km s⁻¹. The radio galaxy has mass $M \lesssim 6 \times 10^9 M_\odot$ and infrared luminosity $L_{\text{IR}} \sim 3 \times 10^{11} L_\odot$ close to its dust Eddington limit, so it is vulnerable to further mass loss from radiative feedback.

Subject headings: black hole physics — galaxies: active — galaxies: clusters: individual (ZwCl 8193)
— galaxies: interactions — galaxies: nuclei — galaxies: peculiar

1. INTRODUCTION

The term “active galactic nucleus” (AGN) reflects the fact that the supermassive black hole (SMBH) powering an AGN is normally found in the nucleus of its host galaxy because dynamical friction against the surrounding stars eventually drives any offset SMBH to the bottom of the galaxy’s gravitational potential well. However, the stellar bulge of nearly every massive galaxy contains a SMBH (Ferrarese & Ford 2000), so hierarchical merging of galaxies should produce stellar bulges initially containing two or more SMBHs that are offset in position and velocity. Following a merger, a pair of inspiraling SMBHs may spend $\sim 10^8$ yr at separations $\gtrsim 1$ kpc (Begelman et al. 1980) before forming a tight binary that could either stall at ~ 1 pc separation or merge. Anisotropic gravitational radiation emitted during a SMBH merger may kick the merged SMBH out of the nucleus into a nearly radial orbit with kpc size for up to $\sim 10^8$ yr before it settles down (Hoffman & Loeb 2007; Gualandris & Merritt 2008). Recoiling SMBHs on

highly eccentric orbits spend most of their time with velocity offsets too small to detect spectroscopically, so Gualandris & Merritt (2008) suggested “an alternative approach would be to search for linear displacements between the AGN emission and the peak of the stellar surface brightness.” Finally, Governato et al. (1994) proposed the existence of “wandering” SMBHs: “If a galaxy is tidally disrupted before coalescence is completed, a possibility exists that its BH will remain naked” for a few Gyr. We have found what we believe is the first example of a nearly naked SMBH in the surviving core of a tidally stripped galaxy.

The discovery program that found the offset SMBH is outlined in Section 2. The radio, optical, and infrared identifications of the offset SMBH and its host galaxy are presented in Section 3, and their long-slit optical spectra are described in Section 5. Section 6 gives our interpretation of the data in terms of a nearly naked SMBH clothed only by the compact remnant of a radio galaxy that was tidally shredded by the brightest cluster galaxy (BCG) in the cluster ZwCl 1715.5+4229 (B1950 coordinate name). This cluster is usually called ZwCl 8193 in the literature.

2. FINDING OFFSET SMBHs

jcondon@nrao.edu

¹The National Radio Astronomy Observatory is a facility of the National Science Foundation operated under cooperative agreement by Associated Universities, Inc.

To discover SMBHs with small linear offsets from their host galaxy bulges, we need a large sample of nearby galaxies containing SMBHs whose existence and positions are revealed by their compact ($\theta \lesssim 1$ mas) radio emission.

Condon, Broderick, & Yin (in prep) compiled a sample of all Two Micron All-Sky Survey (2MASS) Extended Source Catalog (XSC) galaxies (Jarrett et al. 2000) north of $\delta = -40^\circ$, at Galactic latitudes $|b| > 5^\circ$, and brighter than $K_{20\text{Fe}} = 12.25$ at $\lambda = 2.16 \mu\text{m}$, a wavelength at which luminosity is a good tracer of total stellar mass (Madau 1998) and dust extinction is small enough that the 2MASS positions should be close to the bulge centroids. The XSC rms position errors are $0''.3\text{--}0''.5$ in each coordinate, but we found that the 2MASS Point-Source Catalog (PSC) fitted positions better locate the bulge centers with rms errors $\lesssim 0''.1$ in each coordinate. At the typical angular-size distance $\langle D_A \rangle \sim 200$ Mpc of these bright galaxies, a $\Delta \sim 1$ kpc projected linear offset yields an easily detectable angular offset $\Delta\theta \sim 1''$. Condon, Yin, & Broderick also identified the NRAO VLA Sky Survey (NVSS) (Condon et al. 1998) radio sources that have NVSS/2MASS position differences $\lesssim 15''$.

We observed the stronger NVSS identifications with the Very Long Baseline Array (VLBA) at X band ($\nu = 7.6$ GHz, $\lambda \approx 4$ cm) and we re-analyzed archival VLBA data at 8.4 and 2.3 GHz in a large program covering 1215 radio sources with $S \geq 50$ mJy at 1.4 GHz to image the compact components powered by SMBHs in or near bulge centroids (Petrov et al. 2016, in preparation).

The 2MASS Point-Source Catalog (PSC) absolute radial position errors are Rayleigh distributed with $\sigma \approx 0''.115$ and our VLBA absolute positions have $\sigma \approx 0''.001$, so SMBHs offset by more than $\Delta\theta \sim 0''.4$ should be distinguished from nuclear SMBHs with 99.9% reliability. The observed VLBA minus PSC offsets of SMBHs detected before 2014 are consistent with the expected position uncertainties (Figure 1), confirming that nearly all SMBHs are truly nuclear. However, the compact flat-spectrum radio source B3 1715+425 (B1950 coordinate name) is offset by $\Delta\theta > 2''$ from the infrared source 2MASX 17171926+4226571 (J2000 coordinate name).

3. RADIO, OPTICAL, AND INFRARED IDENTIFICATIONS IN ZWCL 8193

The BCG in ZwCl 8193 is the 2MASS galaxy 2MASX 17171926+4226571 at PSC position J2000 $\alpha = 17^{\text{h}} 17^{\text{m}} 19^{\text{s}}.245$, $\delta = +42^\circ 26' 57''.48$. Its $S_{1.4\text{GHz}} = 133.5 \pm 4.0$ mJy NVSS counterpart NVSS J171719+422659 at J2000 $\alpha = 17^{\text{h}} 17^{\text{m}} 19^{\text{s}}.18 \pm 0''.04$, $\delta = +42^\circ 26' 59''.6 \pm 0''.6$ is $> 2''$ north of the BCG. This radio source was first detected at $S = 0.2$ Jy in the 408 MHz Bologna B3 survey (Ficarra et al. 1985) and named B3 1715+425 (equinox B1950 IAU format name). Its 4.85 GHz counterpart is 87GB 1715+4230 (B1950 name) with flux density $S = 134 \pm 16$ mJy (Gregory & Condon 1991). Its flat spectral index $\alpha(1.4, 4.85) \approx 0$ is usually a signature of synchrotron self-absorption in a high-brightness ($T_b \sim 10^{11}$ K) radio component.

Allen et al. (1992) associated 87GB 1715+4230 with the BCG in ZwCl 8193, for which they reported both a stellar absorption-line redshift $z_a = 0.1754 \pm 0.0006$ and a significantly higher emission-line redshift $z_e = 0.1829 \pm 0.0001$. In a flat Λ CDM universe with $H_0 =$

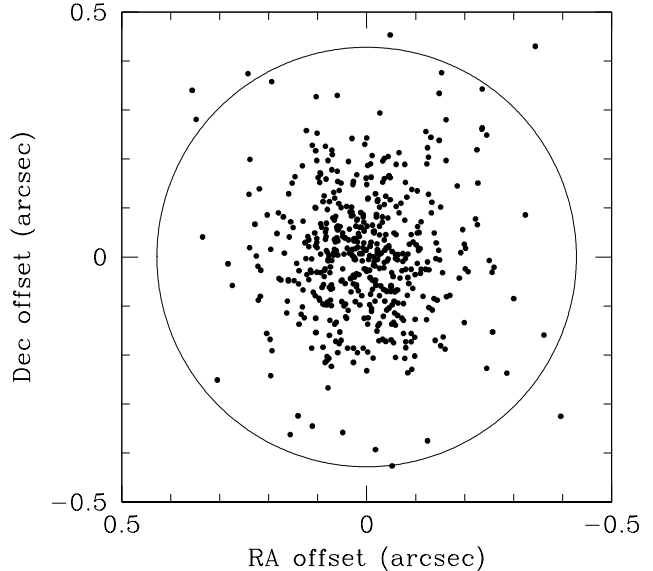


Figure 1. VLBA (SMBH) minus 2MASS PSC (stellar bulge) position offsets of 492 nearby galaxies detected by the VLBA before 2014. The circle with radius $0''.428$ should contain 99.9% of the galaxies if there are no offset SMBHs and the offsets are Rayleigh distributed with $\sigma = 0''.115$. Most of the points just outside the circle are large spiral galaxies whose stellar bulges are partially obscured by dust at $\lambda = 2.16 \mu\text{m}$. B3 1715+425 lies well outside the plotted region.

$70 \text{ km s}^{-1} \text{ Mpc}^{-1}$ and $\Omega_M = 0.3$, $z_a = 0.1754$ implies that the BCG in ZwCl 8193 is at angular-size distance $D_A \approx 613$ Mpc and $1'' \approx 2.97$ kpc. The corresponding luminosity distance is $D_L = (1 + z_a)^2 D_A \approx 850$ Mpc.

Because ZwCl 8193 is a bright X-ray source and “emission-line nebulae are frequently found surrounding the central galaxy in clusters with cooling flows,” Allen et al. (1992) believed “that photoionization by an active nucleus or other activity associated with the radio emission is unlikely to be the principal mechanism for generating the line emission.” Consequently they did not search for the separate radio galaxy responsible for the offset emission-line redshift. Wilman et al. (2006) presented an integral-field $\text{H}\alpha + [\text{N II}]$ line-intensity image showing emission north of the BCG, but they did not discuss the radio source. O’Dea et al. (2010) first noted the compact radio source “is 3 arcsec from the center of the BCG at the location of FUV-bright debris features and may be associated with a merging galaxy,” but associated the diffuse $\text{Ly}\alpha$ emission with ZwCl 8193. Thus the literature has remained unclear and the optical identification of B3 1715+425 is still listed as ZwCL 8193 in the NASA/IPAC Extragalactic Database (NED).

3.1. VLBA Images of B3 1715+425

Bourda et al. (2011) observed B3 1715+425 = J1717+4226 with the VLBA+European VLBI Network at 8.4 and 2.3 GHz on 2008 March 7, and Petrov (2011) determined its position with milliarcsecond accuracy using these data.

We used eight of the ten VLBA stations to reobserve B3 1715+425 in left circular polarization (LCP) at 7.6 GHz (X band) and 4.4 GHz (C band, with the new wideband receiver for improved sensitivity) simultaneously for 4 hours on 2013 December 6. The missing

stations were FD (broken motor) and KP (no fringes for an unknown reason). Half of the IFs were centered on 4.4 GHz and half on 7.6 GHz, and the total data rate was 2048 Mbit/s. Our 7.6 GHz image of B3 1715+425 is shown in Figure 2 and our 4.4 GHz image is shown in Figure 3. The position of the strong central component in this compact symmetric radio source derived from all VLBI observations is J2000 $\alpha = 17^{\text{h}} 17^{\text{m}} 19^{\text{s}}.209641$, $\delta = +42^{\circ} 26' 59''.84514$ with rms uncertainties $\sigma_{\alpha} = 0^{\text{s}}.00001$ and $\sigma_{\delta} = 0^{\text{''}}.0002$, a highly significant $0^{\text{''}}.40 \pm 0^{\text{''}}.12$ west and $2^{\text{''}}.37 \pm 0^{\text{''}}.12$ north of the 2MASS PSC position.

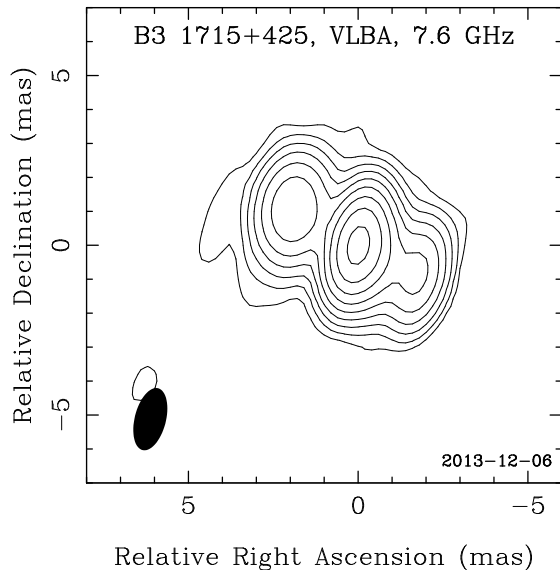


Figure 2. VLBA X-band (7.6 GHz) natural-weighting image of B3 1715+425 with contours plotted at $156 \mu\text{Jy beam}^{-1} \times 1, 2, 4, 8, 16, 32, 64, 128, \text{ and } 256$. The recovered flux density is 77 mJy and the core peak intensity is 52 mJy beam^{-1} . The restoring beam half-power ellipse ($0^{\text{''}}.00188 \times 0^{\text{''}}.00092$ in $PA = -14^{\circ}$) is drawn in the lower left corner.

The central component has a peak intensity $S_p = 52 \text{ mJy beam}^{-1}$ in our 7.6 GHz VLBA image. We approximated the central component by a circular Gaussian and directly fit the observed fringe amplitude distribution as a function of projected baseline length in the (u, v) plane to determine its angular diameter. With this technique and our low rms noise levels $\sim 0.2 \text{ mJy beam}^{-1}$ at X band and $\sim 0.1 \text{ mJy beam}^{-1}$ at C band, we could resolve the central component by the Kovalev et al. (2005) criterion and measure its FWHM diameter $\theta \sim 0^{\text{''}}.0002$. The corresponding quantities at 4.4 GHz are $S_p = 43 \text{ mJy beam}^{-1}$ and $\theta \sim 0^{\text{''}}.0004$. The central component has rest-frame luminosity $L_{9 \text{ GHz}} \approx 6 \times 10^{24} \text{ W Hz}^{-1}$ calculated from our 7.6 GHz measurements, linear diameter $\sim 1 \text{ pc}$, and rest-frame brightness temperature $T_b \sim 3 \times 10^{10} \text{ K}$.

Figure 4 shows how the spectral index $\alpha(4.4, 7.6)$ varies across B3 1715+425. To construct a spectral-index image, we restored both the C- and X-band images with the C-band natural-weight beam and aligned them on the northeastern optically thin region using the two-dimensional cross-correlation technique described by Hovatta et al. (2012) and Pushkarev et al. (2012). At 4.4 GHz the northeastern jet and southwestern counter-

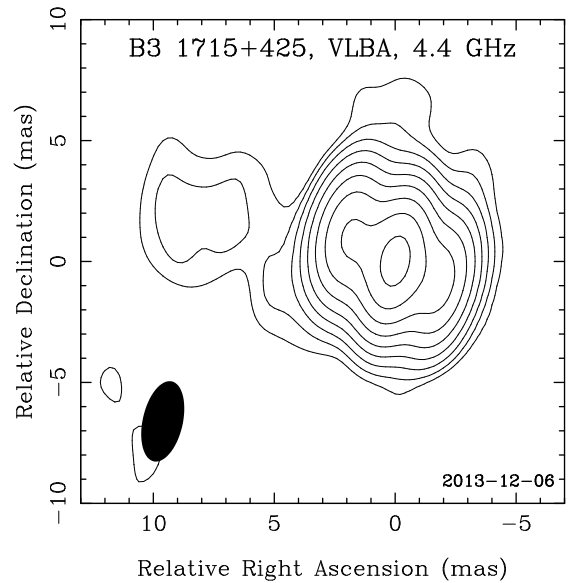


Figure 3. VLBA C-band (4.4 GHz) natural-weighting image of B3 1715+425 with contours plotted at $129 \mu\text{Jy beam}^{-1} \times 1, 2, 4, 8, 16, 32, 64, 128, \text{ and } 256$. The recovered flux density is 84 mJy and the core peak intensity is 43 mJy beam^{-1} . The restoring beam half-power ellipse ($0^{\text{''}}.00339 \times 0^{\text{''}}.00166$ in $PA = -13^{\circ}$) is drawn in the lower left corner.

jet flux densities are 21 mJy and 12 mJy , respectively; at 7.6 GHz they are 14 mJy and 8 mJy .

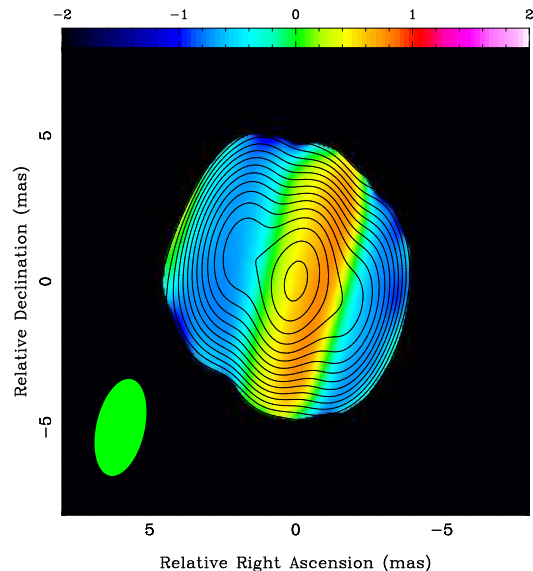


Figure 4. Matched-resolution VLBA spectral-index image of B3 1715+425 uses the C-band natural-weighting restoring beam shown in Figure 3 at both frequencies (green ellipse). The spectral index $\alpha(4.4, 7.6)$ is encoded by the color bar on the top.

The spectral index of the central component was $\alpha(2.3, 8.4) = -0.26 \pm 0.07$ at epoch 2008.2 (Petrov 2011) and $\alpha(4.4, 7.6) = +0.24 \pm 0.13$ at epoch 2013.9, indicating synchrotron self-absorption in a high-brightness core. The spectral-index maximum $\alpha \sim +0.75$ appears $\sim 0^{\text{''}}.001$ southwest of the nucleus. The symmetric jets or lobes have the “normal” steep spectra $-0.9 < \alpha(4.4, 7.6) < -0.7$ of transparent synchrotron sources. We associate the central radio component

with the apparent base of the jet near the SMBH itself (Blandford & Königl 1979) because of its compactness, high brightness temperature, and flat spectrum. Its brightness temperature and spectrum are consistent with a self-absorbed synchrotron source having a nearly equipartition magnetic field strength, as discussed by Readhead (1994). The radio source is too luminous and far too bright to be powered by anything but a SMBH. All known star-forming galaxies have $\nu \approx 8$ GHz brightness temperatures $T_b < 10^{4.5}$ K (Condon et al. 1991).

The symmetric source in Figure 2 is $\sim 0''.005 \approx 15$ pc in projected length, so B3 1715+425 may be a compact symmetric object (CSO) as defined by Wilkinson et al. (1994). The two steep-spectrum components about $0''.002$ from the core at position angles 60° and 245° can be interpreted as a weak jet and a counter-jet of approximately equal flux density, so they are not relativistically beamed. Thus the line between them need not be close to the line of sight (Scheuer & Readhead 1979) and their actual lengths probably are not much greater their projected lengths. Conway et al. (1992) noted that CSOs usually have compact self-absorbed cores with spectra peaking in the GHz frequency range, but these core sources are probably not relativistically boosted (else triple CSOs would be outnumbered by misaligned coreless compact double sources in radio surveys), so their flux densities can be used to calculate their intrinsic brightness temperatures and luminosities. The low polarization of NVSS J171719+422659 (fractional polarization 3σ upper limit $< 0.9\%$) is also typical of CSOs (Gugliucci et al. 2007).

3.2. The Radio Galaxy Originally Identified with B3 1715+425

The full extent of the bloated BCG in the massive cluster ZwCl 8193 is apparent in the deep HST F606W (center $\lambda \approx 606$ nm) wideband ($480 \text{ nm} < \lambda < 710 \text{ nm}$) image (O’Dea et al. 2010) downloaded from the Hubble Legacy Archive (HLA) and shown in Figure 5; it is at least $30'' \approx 90$ kpc at $z_a = 0.1754$. The + marks the HST position of the BCG core and the \times marks the VLBA position of the radio source. Several arcs of gravitationally lensed background galaxies surround it.

Figure 6 covers the white box in Figure 5 with a shallower transfer function to reveal the core of the BCG, several cluster galaxies, and what O’Dea et al. (2010) variously described as a dust lane plus “apparent FUV bright debris features,” and thus the radio source “may be associated with a merging galaxy.” On this HST image, our Gaussian fits give the BCG core position J2000 $\alpha = 17^h 17^m 19^s 231$, $\delta = +42^\circ 26' 57''.05$ and the circled object is at J2000 $\alpha = 17^h 17^m 19^s 202$, $\delta = +42^\circ 26' 59''.90$, only $\Delta\theta = 0''.10$ from the VLBA position.

Our VLBA images reveal no radio emission brighter than 1 mJy beam at the position of the BCG. FIRST (Becker et al. 1995) ($5''.4$ FWHM resolution) does not resolve B3 1715+425, and the FIRST flux density $S \approx 132.5$ mJy equals the NVSS ($45''$ FWHM resolution) flux density $S = 133.5 \pm 4.0$ mJy, so B3 1715+425 has very little or no extended radio emission on angular scales between $5''.4$ and $45''$. The $2''.8$ angular separation between B3 1715+425 and the BCG is smaller than the FIRST beam, so the BCG might be a fairly compact radio source, smaller than the FIRST beam but large

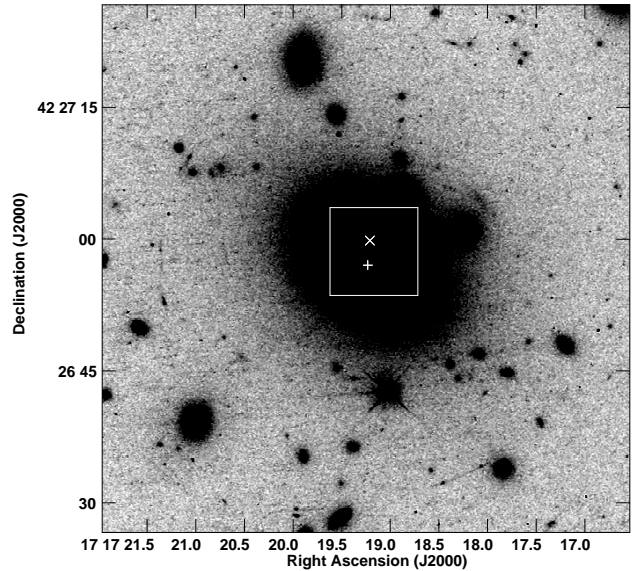


Figure 5. This deep HST F606W image of the galaxy cluster ZwCl 8193 shows the full extent of the BCG and some of its gravitationally lensed background galaxies. The white \times marks the VLBA radio position, the white $+$ marks the HST optical position of the BCG core, and the white box bounds the zoomed image in Figure 6.

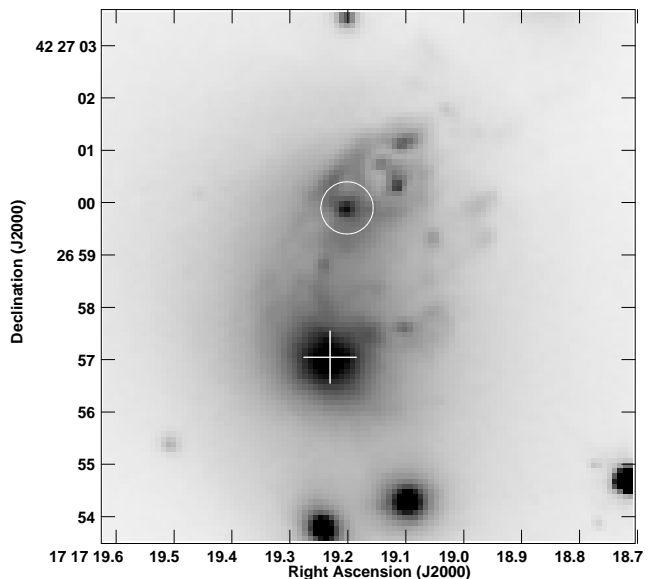


Figure 6. This shallower zoomed HST F606W image of ZwCl 8183 reveals the core of the BCG, the radio galaxy, several cluster galaxies, and extended interaction debris. The HST position of the BCG core is marked by the white $+$, and our new optical identification of B3 1715+425 is enclosed by a white circle centered on its HST position. The HST and VLBA positions coincide within $0''.1$.

enough to be resolved out by the VLBA. In that case, the FIRST position of B3 1715+425 would be at the flux-weighted centroid of the BCG and VLBA positions. The FIRST declination is only $\Delta\theta = 0''.14 \pm 0''.10$ south of the VLBA declination while the BCG and VLBA positions are separated by about $2''.8$, so the BCG likely contributes $< 5\%$ to the total flux density of B3 1715+425.

We conclude that the correct optical identification of the radio source B3 1715+425 is *only* the circled object, and not the BCG nucleus $2''.85 \approx 8.5$ kpc to the south or other tidal debris. The 2MASX infrared source is a marginally significant $\Delta\theta \sim 0''.43$ north of the optical BCG nucleus, which is consistent with the $\lambda = 2.16 \mu\text{m}$ source being a blend of emission from the BCG and material to the north.

The compact galaxy that we call the unique optical identification of B3 1715+425 is listed in the HLA catalog with F606W AB magnitude $m = 21.417 \pm 0.048$ measured through a $0''.3$ radius circular aperture. At distance modulus $m - M = 39.64$, its absolute red magnitude is $M_r \approx -18.2$. Its concentration index is $CI = 1.794$, so it is flagged as extended ($CI > 1.3$). A Gaussian fit on the HST F606W image yields a half-power ellipse $0''.39 \times 0''.30$ in size while stars of comparable magnitude appear as $0''.25$ FWHM circles, so the deconvolved FWHM size of the galaxy hosting B3 1715+425 is only $0''.3 \times 0''.2 \sim 0.9 \text{ kpc} \times 0.6 \text{ kpc}$. Thus this radio galaxy is much smaller and less luminous than the $(0.3 \rightarrow 1)L^*$ elliptical galaxies identified with other CSOs (Readhead et al. 1996) or comparably luminous radio sources.

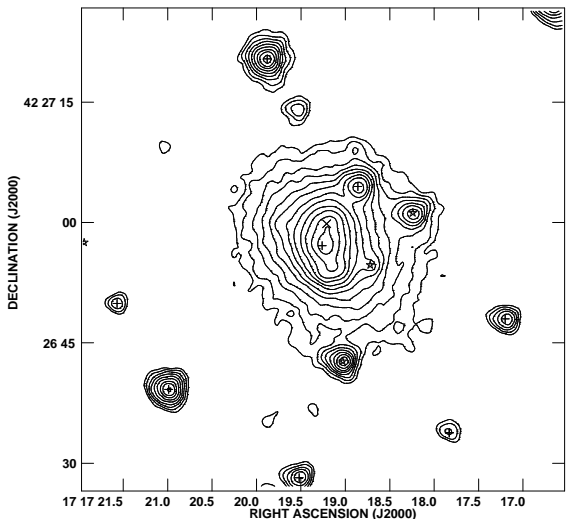


Figure 7. IRAC1 ($\lambda = 3.6 \mu\text{m}$) contour image of ZwCl 8193. At $\lambda = 3.6 \mu\text{m}$ the brightness is greatest at the position of the BCG nucleus (marked by the + at the image center). Successive contours are $0.10 \text{ MJy sr}^{-1} \times 2^0, 2^{1/2}, 2^1, 2^{3/2}, \dots$ above the background.

3.3. Infrared Sources in ZwCl 8193

The infrared structure of ZwCl 8193 is resolved in archival Spitzer IRAC images (Quillen et al. 2008) downloaded from the NASA/IPAC Infrared Science Archive (IRSA) in IRAC Bands 1 ($\lambda \approx 3.6 \mu\text{m}$, $\theta \approx 1''.9$ FWHM resolution) and 4 ($\lambda \approx 8 \mu\text{m}$, $\theta \approx 2''.8$ FWHM), and it is marginally resolved in the MIPS-24 ($\lambda \approx 24 \mu\text{m}$, $\theta \approx 6''.4$ FWHM) image. Infrared contour plots covering the same area as Figure 5 are shown in Figures 7, 8, and 9. The near- and mid-infrared images help to distinguish between Galactic stars (\star), cluster galaxies (+), and the radio galaxy (\times). Individual stars and dustless galaxies of stars have temperatures $T \gtrsim 3500 \text{ K}$ and

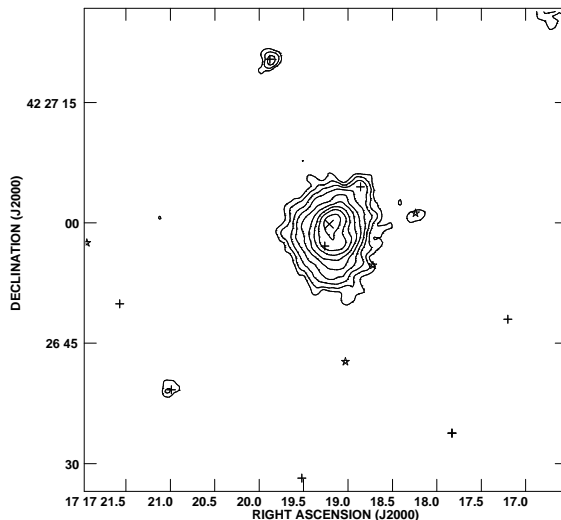


Figure 8. IRAC4 ($\lambda = 8 \mu\text{m}$) contour image of Zw 8193. The radio source position (\times) is brighter than the BCG nucleus. Successive contours are $0.25 \text{ MJy sr}^{-1} \times 2^0, 2^{1/2}, 2^1, 2^{3/2}, \dots$ above the background.

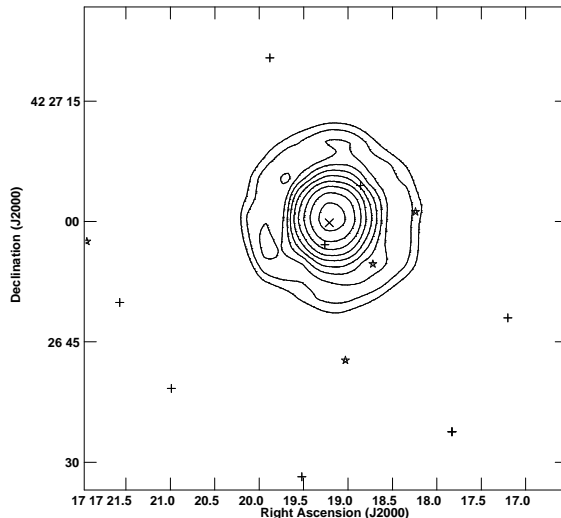


Figure 9. MIPS-24 ($\lambda = 24 \mu\text{m}$, $\theta \approx 6''$ FWHM resolution) contour image of Zw 8193. Stars and galaxies are nearly invisible, and the centroid is near the radio position marked by the \times . Successive contours are $0.20 \text{ MJy sr}^{-1} \times 2^0, 2^{1/2}, 2^1, 2^{3/2}, \dots$ above the background.

Wien peak wavelengths $\lambda_w \lesssim 1 \mu\text{m}$, so they are significantly brighter in Band 1 than in Band 4, and they have disappeared in MIPS-24. In Band 1, the BCG nucleus (+) is brighter than the radio galaxy (\times), but the radio source position marks the highest brightness in the whole Band 4 field, and at $\lambda = 24 \mu\text{m}$ it is completely dominant, as indicated by the MIPS-24 position J2000 $\alpha = 17^{\text{h}} 17^{\text{m}} 19^{\text{s}} 17$, $\delta = +42^{\circ} 27' 00''.5$ determined by a Gaussian fit. Quillen et al. (2008) noted that ZwCl 8193 has a strong mid-IR excess compared with a quiescent elliptical galaxy. Such excess emission is usually produced by warm interstellar dust at temperatures $T \ll 3500 \text{ K}$. We identify the mid-infrared source in ZwCl 8193 *only* with the radio galaxy and its surrounding debris, and not with the elliptical BCG in ZwCl 8193.

From the MIPS image we measured a $\lambda = 24 \mu\text{m}$

($\nu = 1.25 \times 10^{13}$ Hz) flux density $S_{24\mu\text{m}} \approx 10 \pm 1$ mJy. The $\lambda = 70\mu\text{m}$ ($\nu \approx 4.3 \times 10^{12}$ Hz) flux density of the radio galaxy is $S_{70\mu\text{m}} \approx 177$ mJy (Quillen et al. 2008), and the ratio $S_{70\mu\text{m}}/S_{24\mu\text{m}} \sim 20$ is typical of galaxies selected at $\lambda = 70\mu\text{m}$ (Clements et al. 2011). Thus the mid-infrared luminosity of the radio galaxy is $\nu L_\nu \approx 3 \times 10^{10} L_\odot$ at $\lambda = 24\mu\text{m}$, and its total infrared luminosity may be up to $10\times$ higher, $L_{\text{IR}} \sim 3 \times 10^{11} L_\odot$. We cannot rule out a minor contribution by the BCG to the $70\mu\text{m}$ luminosity because the $70\mu\text{m}$ resolution is inadequate ($\theta \approx 20''$ FWHM) to distinguish the radio galaxy from the BCG.

The steep spectrum between $24\mu\text{m}$ and $70\mu\text{m}$ indicates a low dust temperature $T_d < 100$ K. The specific intensity of the dust source cannot exceed that of a $T = T_d < 100$ K blackbody, so the combination of high luminosity and low temperature implies that the diameter of the dust source is at least

$$D_d > \left(\frac{L_{\text{IR}}}{\pi\sigma T_d} \right)^{1/2} \sim 100 \text{ pc} , \quad (1)$$

where $\sigma \approx 5.67 \times 10^{-5} \text{ erg s}^{-1} \text{ cm}^{-2} \text{ K}^{-4}$ is the Stefan-Boltzmann constant. Thus the dust source is much larger than the SMBH accretion disk. The dust may well be heated by the SMBH; the stars in the optically faint radio galaxy and surrounding debris can contribute significantly to the high infrared luminosity only if they are young, massive, and heavily obscured at visible wavelengths, as in the case of Arp 220.

4. X-RAY SOURCES

The X-ray source 1RXS J171718.9+422652 at J2000 $\alpha = 17^{\text{h}} 17^{\text{m}} 18^{\text{s}}.9$, $\delta = +42^\circ 26' 52''$ overlaps ZwCl 8193 (Massaro et al. 2009), the BCG, and the radio galaxy. Its 0.1–2.4 keV flux $2.03 \times 10^{-12} \text{ erg cm}^{-2}$ corresponds to a soft X-ray luminosity $\approx 1.7 \times 10^{44} \text{ erg s}^{-1}$ at the 850 Mpc luminosity distance of the cluster.

We observed ZwCl 8193 with the *Chandra X-ray Observatory* on 2013 October 7 using the ACIS S3 chip in a timed exposure “faint” mode as part of program GO3-14112X. The nominal integration time was 18202 s. We reprocessed and reduced the observations using CIAO 4.8 and calibration files CALDB 4.7.2. Data were filtered for background flares and restricted to the energy range 0.5–7 keV.

Figure 10 shows the 0.5–7 keV *Chandra* image with the radio source and BCG marked. An X-ray peak coincides with the radio source and is clearly distinguishable from the extended X-ray emission associated with the cluster or BCG. Wavelet detection succeeds in identifying the unresolved X-ray source with centroid J2000 $\alpha = 17^{\text{h}} 17^{\text{m}} 19^{\text{s}}.22$, $\delta = +42^\circ 26' 59''.6$, but measuring the X-ray counts in the presence of the highly structured extended emission required custom photometry that is highly uncertain. We therefore did not attempt to model the source spectrum or correct for absorption.

While the X-ray properties of the BCG are highly uncertain, the detection of an unresolved X-ray source coincident with the radio source is significant. We detected 85 ± 15 counts and a count rate of $0.0047 \pm 0.0008 \text{ s}^{-1}$ in the 0.5–7 keV range (statistical errors only). The flux is $(3.6 \pm 0.6) \times 10^{-14} \text{ erg cm}^{-2} \text{ s}^{-1}$, and the 0.5–7 keV X-ray

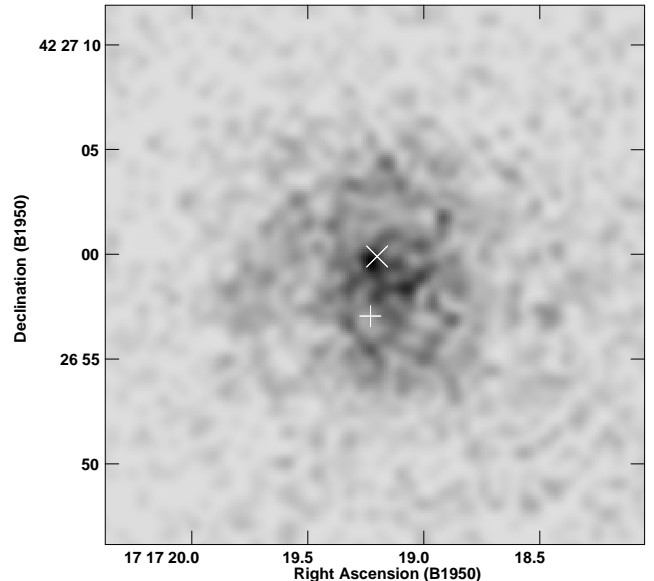


Figure 10. The white \times marks the VLBA radio position of B3 1715+425, and the white $+$ marks the HST optical position of the BCG core in this *Chandra* 0.5–7 keV X-ray image. The detection of the unresolved X-ray source on the radio position is significant, and there is no compact source visible on the BCG position.

luminosity is $(3.1 \pm 0.5) \times 10^{42} \text{ erg s}^{-1}$ (again, all errors are statistical and do not include the systematic errors arising from separating the compact from the extended emission).

5. LONG-SLIT SPECTROSCOPY OF ZWCL 8193

After Allen et al. (1992) reported an emission-line redshift $z_e = 0.1829$ that they associated with the BCG in ZwCl 8193, Edge et al. (2002) imaged the faint Pa α emission connecting the BCG and B3 1715+425 and estimated a velocity difference between them of $\sim 400 - 500 \text{ km s}^{-1}$. We observed ZwCl 8193 using the Double Imaging Spectrograph on the Astrophysical Research Consortium (ARC) 3.5 m telescope at the Apache Point Observatory on 17 April 2012. The long slit was $1''.5$ wide and oriented north-south to include both B3 1715+425 and the BCG (Figure 11). We obtained red (resolution $R \sim 3250$) and blue ($R \sim 2400$) spectra from the UV atmospheric cutoff to 9800 \AA that included H α 6563, the [N II]6549,6583 doublet, H β 4861, the [O III]4959,5007 doublet, and [O III]4363 in emission plus the Ca II H and K $\lambda = 3968, 3934 \text{ \AA}$ lines in absorption. Eight 600 s exposures were flat-fielded, wavelength-calibrated, rectified, sky-subtracted, and median combined. The absolute velocity uncertainties are $\sim 150 \text{ km s}^{-1}$, but the relative uncertainties are only $\sim 10 \text{ km s}^{-1}$ for bright emission lines. The Ca II H and K lines confirm the Allen et al. (1992) absorption line redshift toward the BCG, and the [O III]4363 line confirms the reported offset between absorption-line and emission-line redshifts.

A contour plot of the H α and [N II] line intensities is shown in Figure 12, with north pointing down. The H α emission-line redshift varies from $z_1 \approx 0.18215$ near the BCG nucleus at $\Delta\delta \approx -2''.85$ to $z_2 \approx 0.18271$ at the declination of B3 1715+425 ($\Delta\delta \equiv 0$), for a redshift difference $\Delta z = (z_2 - z_1)/(1 + z_1) \approx 0.00047$ and a radial

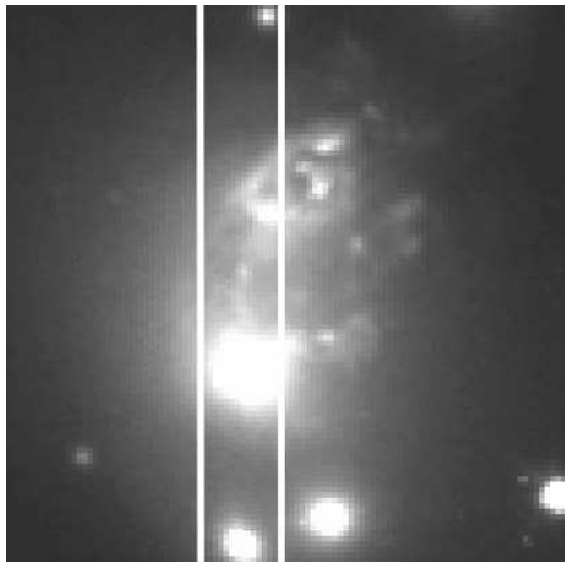


Figure 11. The $1''.5$ wide spectrograph slit between the vertical white lines includes the radio galaxy, the BCG, and the region between them.

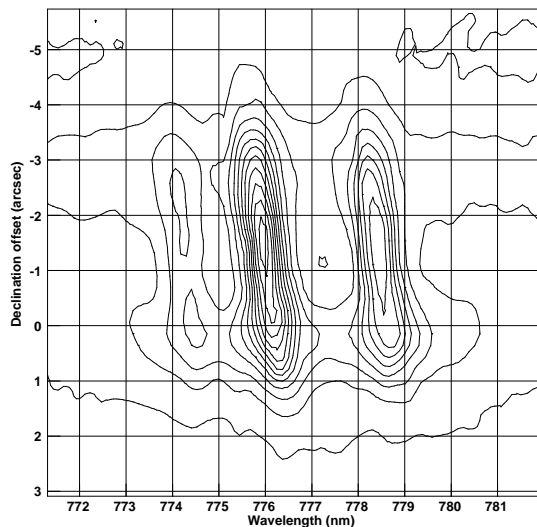


Figure 12. Contour plot of the emission-line spectrum centered on the $H\alpha$ and adjacent $[\text{N II}]$ lines. Successive contours are separated by the same linear interval in brightness (arbitrary units). Abscissa: Wavelength (nm). Ordinate: Declination offset from the optical counterpart of B3 1717+425; note that north is down. The BCG nucleus is at $\Delta\delta = -2''.85$, and its continuum emission is visible as the horizontal band centered on that declination offset.

velocity difference of only $v \approx cz \approx 140 \text{ km s}^{-1}$. The difference between the emission-line redshift $z_e = 0.18271$ of B3 1715+425 and the absorption-line redshift $z_a = 0.1754$ of the BCG galaxy is $\Delta z_{ea} = (z_e - z_a)/(1 + z_a) \approx 0.0062$, so the ionized gas in B3 1715+425 is moving away from the BCG with a radial speed $v_r \approx cz \approx 1860 \text{ km s}^{-1} \gg 140 \text{ km s}^{-1}$. The FWHM width of the $H\alpha$ line is $\Delta v \approx 480 \text{ km s}^{-1}$ near B3 1715+425 and falls to $\Delta v \lesssim 320 \text{ km s}^{-1}$ midway between B3 1715+425 and the BCG. These features are very similar to those of the disk and ionized tail of the galaxy ESO 137-001 that is undergoing ram-pressure stripping as it falls into the Norma cluster (Fossati et al. 2016), so all of the emission-line gas appears to have originated in B3 1715+425, and

we use $v_r \approx 1860 \text{ km s}^{-1}$ as the radial velocity of B3 1715+425 relative to the BCG.

The diagnostic emission-line intensity ratios $\log([\text{N II}]/H\alpha) \approx -0.2$ and $\log([\text{O III}]/H\beta) \approx -0.15$ lie in the “composite” range of the BPT diagram (Kewley et al. 2006), suggesting that much of the line emission is from photoionization by stars. The far weaker $[\text{O III}]4363$ emission indicates little ionization by strong shocks.

6. INTERPRETATION

We unambiguously identify the compact and luminous radio source B3 1715+425 with a uniquely small and optically faint radio galaxy at least 8.5 kpc from the nucleus of the BCG in ZwCl 8193. An ionized wake extends from the radio galaxy to the BCG, suggesting that the radio galaxy is now moving away from the BCG with a radial component of velocity $v_r \approx 1860 \text{ km s}^{-1}$. BCGs can have nuclear escape velocities up to 3000 km s^{-1} (Merritt et al. 2004), so the fleeing radio galaxy may still be gravitationally bound to the BCG and/or the cluster ZwCl 8193.

The SMBH powering the radio source is still $\lesssim 0.1 \text{ kpc}$ from the radio galaxy nucleus, so it must have nearly the same velocity as its host emission-line galaxy. The high SMBH velocity relative to the BCG is consistent with (1) gravitational recoil following the merger of two spinning SMBHs or slingshot ejection of one SMBH from a triple system in the BCG or (2) the velocity of a galaxy that fell into the gravitational potential well in the center of the massive cluster ZwCl 8193.

In case (1), tidal forces would have stripped the SMBH of its surrounding stars and dark matter just prior to a merger (Hoffman & Loeb 2007). The violent jerk of post-merger gravitational-wave recoil or slingshot ejection would have left behind most of what remained, so the initially naked SMBH would have to accrete the small but finite ($\sim 0.9 \text{ kpc} \times 0.6 \text{ kpc}$) radio galaxy we see today while leaving the BCG at speeds $v \gtrsim 2 \times 10^3 \text{ km s}^{-1}$. The speeding SMBH can accrete only the stars, dark matter, and gas that lie within an impact parameter b below which the gravitational potential energy (GM/b) of the SMBH is greater than the kinetic energy per unit mass $v^2/2$ of the accreted matter, so

$$\left(\frac{b}{\text{pc}}\right) \approx 2.2 \left(\frac{M}{10^9 M_\odot}\right) \left(\frac{v}{2000 \text{ km s}^{-1}}\right)^{-2}. \quad (2)$$

The velocity dispersion or rotational velocity of the accreted material is only $v_{\text{rot}} \approx \Delta v/2 \approx 240 \text{ km s}^{-1}$ at radial distance $r \approx 450 \text{ pc}$ from the SMBH, indicating that the total mass of the radio galaxy including its SMBH is not more than $M \approx rv_{\text{rot}}^2/G$, or

$$\left(\frac{M}{10^9 M_\odot}\right) \lesssim 6.0 \left(\frac{r}{450 \text{ pc}}\right) \left(\frac{v_{\text{rot}}}{240 \text{ km s}^{-1}}\right)^2. \quad (3)$$

Inserting $M \lesssim 6 \times 10^9 M_\odot$ from Equation 3 into Equation 2 yields $b \lesssim 10 \text{ pc}$, which is much smaller than the radius of the galaxy surrounding the SMBH. We conclude that any SMBH violently ejected from the BCG nucleus with velocity $v \gtrsim 2000 \text{ km s}^{-1}$ could not have accreted the extended galaxy that currently surrounds it.

This leaves case (2), a formerly normal galaxy that fell into ZwCl 8193, was tidally stripped as it passed near the BCG nucleus, and is now rapidly moving away from the BCG. Only the SMBH and the small central portion of that galaxy denser than the BCG core remain intact, with total mass $M \lesssim 6 \times 10^9 M_\odot$ and radius $r \sim 450$ pc. Such severe stripping requires a relatively rare collision with impact parameter $b \lesssim 1$ kpc, the core radius of the most massive elliptical galaxies (Faber et al. 1997). The path of the escaping galaxy is traced by its ionized tail, the velocity of the escaping galaxy is probably close to the cluster escape velocity, and the small velocity gradient along that tail is caused by gas drag from the ISM of the BCG. The outer portion of the stripped galaxy now appears as “debris” north of the BCG nucleus in Figure 6.

Finally, most massive bulges contain nuclear SMBHs, and the typical bulge/SMBH mass ratio is ~ 500 (McConnell & Ma 2013). Heavy stripping significantly reduces this ratio, making low-mass stripped galaxies surrounding massive SMBHs more vulnerable to additional mass loss caused by “quasar mode” radiative feedback. The $L_{\text{IR}} \sim 3 \times 10^{11} L_\odot$ total infrared luminosity of our $M \lesssim 6 \times 10^9 M_\odot$ stripped galaxy is well below its classical Eddington limit ($L_E/L_\odot \approx 3.3 \times 10^4 (M/M_\odot) \lesssim 2 \times 10^{14}$ caused by radiation pressure from Thomson scattering in ionized hydrogen gas. However, the radiation pressure per unit mass from dust scattering can be up to 500 times larger (Fabian et al. 2008), so the luminosity of our stripped galaxy may be close to its dust Eddington limit $L_D \lesssim 4 \times 10^{11} L_\odot$.

This work is based on observations made at the Apache Point Observatory, operated by New Mexico State University. The scientific results reported in this article are based on observations made with the Chandra X-ray Observatory. Support for this work was provided by the National Aeronautics and Space Administration through Chandra Award Number GO3-14112X issued by the Chandra X-ray Observatory Center, which is operated by the Smithsonian Astrophysical Observatory for and on behalf of the National Aeronautics Space Administration under contract NAS8-03060. This research has made use of software provided by the Chandra X-ray Center (CXC) in the application packages CIAO and ChIPS. This research has made use of the NASA/IPAC Extragalactic Database (NED) and the NASA/IPAC Infrared Science Archive (IRSA), which are operated by the Jet Propulsion Laboratory, California Institute of Technology, under contract with the National Aeronautics and Space Administration. The Hubble Legacy Archive (HLA) is based on observations made with the NASA/ESA Hubble Space Telescope, and obtained from the Hubble Legacy Archive, which is a collaboration between the Space Telescope Science Institute (STScI/NASA), the Space Telescope European Coordinating Facility (ST-ECF/ESA) and the Canadian Astronomy Data Centre (CADCF/NRC/CSA).

Facilities: ARC, CXO, VLBA.

Data for this paper are provided in a persistent repository Chandra ObsId 14988

REFERENCES

- Allen, S. W., Edge, A. C., Fabian, A. C., Bohringer, H., Crawford, C. S., Ebeling, H., Johnstone, R. M., Naylor, T., & Schwarz, R. A. 1992, MNRAS, 259, 67
- Becker, R. H., White, R. L., & Helfand, D. J. 1995, ApJ, 450, 559
- Begelman, M. C., Blandford, R. D., & Rees, M. J. 1980, Nature, 287, 307
- Blandford, R. D., & Königl, A. 1979, ApJ, 232, 34
- Bourda, G., Collioud, A., Charlot, P., Porcas, R. W., Garrington, S. T. 2011, A&A, 526, A102
- Clements, D. L., Bendo, G., Pearson, C., Khan, S. A., Matsuura, S., & Shirahata, M. 2011, MNRAS 411, 373
- Condon, J. J., Huang, Z.-P., Yin, Q. F., & Thuan, T. X. 1991, ApJ, 378, 65
- Condon, J. J., Cotton, W. D., Greisen, E. W., Yin, Q.-F., Perley, R. A., Taylor, G. B., & Broderick, J. J. 1998, AJ, 115, 1693
- Conway, J. E., Pearson, T. J., Readhead, A. C. S., Unwin, S. C., Xu, W., & Mutel, R. L. 1992, ApJ 396, 62
- Edge, A. C., Wilman, R. J., Johnstone, R. M., Crawford, C. S., Fabian, A. C., & Allen, S. W. 2002, MNRAS, 337, 49
- Faber, S. M., Tremaine, S., Ajhar, E. A., et al. 1997, AJ, 114, 1771
- Fabian, A. C., Vasudevan, R. V., & Gandhi, P. 2008, MNRAS, 386, L43
- Ferrarese, L., & Ford, H. 2005, Space Sci Rev, 116, 523
- Ficarra, A., Gruelf, G., & Tomassetti, G. 1985, A&AS, 59 255
- Fossati, M., Fumagalli, M., Boselli, A., Gavazzi, G., Sun, M., & Wilman, D. J. 2016, MNRAS 455, 2028
- Governato, F., Colpi, M., & Maraschi, L. 1994, MNRAS, 271, 317
- Gregory, P. C., & Condon, J. J. 1991, ApJS, 75, 1011
- Gualandris, A., & Merritt, D. 2008, ApJ, 678, 780
- Gugliucci, N. E., Taylor, G. B., Peck, A. B., & Giroletti, M. 2007, ApJ, 661, 78
- Hoffman, L., & Loeb, A. 2007, MNRAS, 377, 957
- Hovatta, T., Lister, M. L., Aller, M. F., Aller, H. D., Homan, D. C., Kovalev, Y. Y., Pushkarev, A. B., & Savolainen, T. 2012, AJ, 144, 105
- Jarrett, T. H., Chester, T., Cutri, R., Schneider, S., Skrutskie, M., & Huchra, J. P. 2000, AJ, 119, 2498
- Kewley, L. J., Groves, B., Kauffmann, G., & Heckman, T. 2006, MNRAS, 372, 961
- Kovalev, Y. Y., Kellermann, K. I., Lister, M. L., et al. 2005, AJ, 130, 2473
- Madau, P., Pozzetti, L., & Dickinson, M. 1998, ApJ, 498, 106
- Massaro, E., Giommi, P., Leto, C., Marchegiani, P., Maselli, A., Perri, M., Piranomonte, S., & Scavi, S. 2009, A&A, 495, 691
- McConnell, N. J., & Ma, C.-P. 2013, ApJ, 764, 184
- Merritt, D., Milosavljević, M., Favata, M., Hughes, S. A., & Holz, D. E. 2004, ApJ, 607, L9
- O’Dea, K. P., Quillen, A. C., O’Dea, C. P., et al. 2010, ApJ, 719, 1619
- Petrov, L. 2011, AJ, 142, 105
- Pushkarev, A. B., Hovatta, T., Kovalev, Y. Y., Lister, M. L., Lobanov, A. P., Savolainen, T., & Zensus, J. A. 2012, A&A, 545, 113
- Quillen, A. E., Zufelt, N., Park, J., O’Dea, C. P., Baum, S. A. et al. 2008, ApJS, 176, 39
- Readhead, A. C. S. 1994, ApJ, 426, 51
- Readhead, A. C. S., Taylor, G. B., Xu, W., Pearson, T. J., Wilkinson, P. N., & Polatidis, A. G. 1996, ApJ, 460, 612
- Scheuer, P. A. G., & Readhead, A. C. S. 1979, Nature, 277, 182
- Wilkinson, P. N., Polatidis, A. G., Readhead, A. C. S., Xu, W., & Pearson, T. J. 1994, ApJ, 432, L87
- Wilman, R. J., Edge, A. C., & Swinbank, A. M. 2006, MNRAS, 371, 93